



| | |
|------------------|---|
| Title | Distinct neural representations of hand movement direction between motor imagery and execution in the presupplementary motor area |
| Author(s) | Yang, Yuxiang; Yang, Huixiang; Imai, Fumihito; Ogawa, Kenji |
| Citation | Neuroscience research, 191, 57-65 https://doi.org/10.1016/j.neures.2023.01.001 |
| Issue Date | 2023-06 |
| Doc URL | http://hdl.handle.net/2115/92521 |
| Rights | ©2023. This manuscript version is made available under the CC-BY-NC-ND 4.0 license http://creativecommons.org/licenses/by-nc-nd/4.0/ |
| Rights(URL) | http://creativecommons.org/licenses/by-nc-nd/4.0/ |
| Type | article (author version) |
| File Information | Yang-Manuscript_with_figure.pdf |



[Instructions for use](#)

1 **Distinct neural representations of hand movement direction between**
2 **motor imagery and execution in the presupplementary motor area**

3

4 Yuxiang Yang^a, Huixiang Yang^b, Fumihito Imai^a, Kenji Ogawa^{a*}

5

6 ^aDepartment of Psychology, Graduate School of Humanities and Human Sciences,

7 Hokkaido University

8 ^bInstitute for Advanced Co-Creation Studies, Osaka University

9

10 *Corresponding author:

11 Dr. Kenji Ogawa

12 Department of Psychology, Graduate School of Humanities and Human Sciences,

13 Hokkaido University, Kita 10, Nishi 7, Kita-ku, Sapporo, 060-0810 Japan

14 Tel/Fax: +81-011-706-4093

15 E-mail: ogawa@let.hokudai.ac.jp.

16

17 Total number of pages: 25

18 Total number of figures: 7

19 Total number of tables: 3

20

1 **Abstract**

2 Motor simulation theory proposes a functional equivalence between motor execution
3 (ME) and its simulation, suggesting that motor imagery (MI) is the self-intentioned
4 simulation of one's actions. This study used functional magnetic resonance imaging
5 (fMRI) with multivoxel pattern analysis to test whether the direction of hand movement
6 is represented with a similar neural code between ME and MI. In our study, participants
7 used their right hand to move an on-screen cursor in the left–right direction with a
8 joystick or imagined the same movement without execution. The results indicated that
9 the left–right direction as well as their modality (ME or MI) could be decoded
10 significantly above the chance level in the presupplementary motor area (pre-SMA) and
11 primary visual cortex (V1). Next, we used activation patterns of ME as inputs to the
12 decoder to predict hand move directions in MI sessions and found a significantly
13 higher-than-chance accuracy only in V1, not in pre-SMA. Moreover, the
14 representational similarity analysis showed similar activation patterns for the same
15 directions between ME and MI in V1 but not in pre-SMA. This study's finding indicates
16 distinct spatial activation patterns for movement directions between ME and MI in pre-
17 SMA.

18

19 **Keywords**

20 motor imagery; motor execution; fMRI; multivoxel classification analysis;
21 representational similarity analysis; presupplementary motor area

22

1 **Introduction**

2 Motor imagery (MI) is a cognitive ability defined as a “mental simulation” of motor
3 execution (ME) without actual action (Decety, 1996; Grush, 2004; Hanakawa, 2016). It
4 has been believed that the neural state of an imagined movement is similar to the state
5 of execution of that action (Jeannerod, 2001). Early neuroimaging studies showed that
6 MI and ME activate roughly the same brain regions (Hanakawa et al., 2008; Munzert et
7 al., 2009). Moreover, a large overlap of regions between MI and ME was found in a
8 meta-analysis study (Hardwick et al., 2018). However, these studies mainly analyzed a
9 single voxel activity or averaged activities within the region and not the activation
10 patterns among multivoxels. Thus, although MI and ME could activate the same brain
11 regions, it remains unclear whether MI and ME use similar neural codes for the same
12 action.

13 Recently, a technique called multivoxel pattern analysis (MVPA) was developed
14 (Weaverdyck et al., 2020). MVPA examines the spatial pattern of brain activations,
15 whereas univariate analyses only consider the overall magnitude of the responses.
16 MVPA studies showed that MI for different types of right-hand actions could be
17 decoded significantly above chance level in M1 and premotor cortices (Pilgramm et al.,
18 2016). Moreover, these different hand actions could also be decoded between MI and
19 ME (cross-model) in premotor cortices. However, in representational similarity analysis
20 (RSA), representational dissimilarity matrices showed that MI and ME represent
21 separate clusters, although the representational organization of action types within these
22 clusters was identical (Zabicki et al., 2017). Therefore, premotor cortices use similar
23 neural codes for different types of hand actions between MI and ME.

24 By contrast, it remains unclear whether the different directions of specific hand

1 action use the same neural code between MI and ME. Ogawa and Inui instructed the
2 participants to perform visually guided movements using a normal mouse and a left–
3 right reversed mouse. Their study showed that the direction of hand movement could be
4 decoded in the hand region of the primary motor area (Mot) (Ogawa & Inui, 2012). Our
5 study thus attempted to decode ME of hand movement direction and investigate whether
6 we could decode MI in motor-related regions.

7 Our study also examined whether the same hand movement, but with different
8 directions in MI and ME used similar neural codes. Our participants first performed the
9 ME tasks by moving their right hand using a joystick to move an invisible cursor to the
10 left or right target. They subsequently performed the MI tasks, imagining the same
11 action as the ME tasks. This experimental design allowed us to compare the activity
12 pattern between ME and MI using multivoxel classification analysis and RSA.

13

14 **Materials and Methods**

15 **Participants**

16 Participants were 17 volunteers (12 females, 5 males) from Hokkaido University, with
17 an average age of 23.18 years (range = 20–26, SD = 1.74). Of these, two female
18 participants were excluded because of excessive head movement during scanning. All
19 participants were right-handed, according to the Edinburgh Handedness Inventory. The
20 sample size was estimated from a prior hand-moving decoding study (Ogawa & Inui,
21 2012) using G*Power version 3.1.9 (Erdfelder et al., 2009; Faul et al., 2007). We used
22 15 participants to get power $(1 - \beta) = .95$, with $\alpha = .05$ and Cohen's $d = 1.03$.

23

24 **Task procedures**

1 All participants completed two practice sessions containing ten trials before three ME
2 sessions and three MI sessions (20 trials per ME and MI session) in a functional
3 magnetic resonance imaging (fMRI) scanner without scanning. Experimental stimuli
4 were controlled by Psychophysics Toolbox Version 3 (PTB-3) (Brainard, 1997; Kleiner
5 et al., 2007; Pelli, 1997) in MATLAB (The MathWorks, Inc.).

6

7 **Practice session**

8 In practice session 1, for each trial, a white fixation was presented in the center of the
9 screen, and above the fixation, there was a countdown from “3” to “1” that lasted 3 s. At
10 the end of the countdown, two squares were presented on the left and right sides of the
11 screen, and the color of the central fixation changed to green or yellow (target phase),
12 indicating the target (green: left square; yellow: right square). Half of the ten trials were
13 green, and the other half was yellow, presented in random order. After 2 s, the color of
14 central fixation changed to red (execution phase). During the execution phase, a joystick
15 cursor (a small white “x”) was presented centrally on the screen. The participants then
16 moved the cursor with their right hand to the target square, which was indicated in the
17 target phase, and maintained the cursor in the target square until the color of the central
18 fixation changed from red to white. The execution phase lasted for 2 s, and then, the
19 cursor was frozen, showing the participants the final position of the cursor in the
20 execution phase for 3 s (result phase). Participants then allowed the joystick to return to
21 its original position and let the joystick bring their right hand back (Figure 1).
22 Participants repeated practice session 1 until getting 100% accuracy. Practice session 2
23 is almost the same as practice session 1. The difference was that in the execution phase
24 of practice session 2, the joystick cursor was not presented. Moreover, it showed the

1 cursor's last position in the execution phase to the participants in the result phase.

2

3 **Execution session**

4 During the execution sessions, participants completed three execution sessions with
5 fMRI scanning. The differences between execution sessions and practice session 2 were
6 that each execution session included 20 trials (half were left, and half were right), and
7 the time of countdown in the countdown phase was from 3 to 9 s (Figure 2).

8

9 **Imagery session**

10 After three execution sessions, participants completed three imagery sessions (20 trials
11 per session). In the imagery session, the execution phase changed to the imagery phase,
12 and the result phase changed to the evaluation phase with the same duration. In the
13 imagery phase, participants imagined that they move the cursor by using the joystick
14 and put the cursor into the target, which was indicated in the target phase, without actual
15 movement. Participants were instructed to use both kinesthetic and visual images before
16 the practice session. After the imagery phase, the participants immediately evaluated the
17 quality of the MI in this trial using their left hand (from 1: very good to 4: very poor). In
18 the evaluation phase, participants were instructed only to choose "4" when they failed to
19 imagine before the practice session, which helped us to exclude the error.

20

21 **MRI acquisition**

22 "All scans were performed on a Siemens (Erlangen, Germany) 3-Tesla Prisma scanner
23 with a 64-channel head coil at Hokkaido University. T2*-weighted echo-planar imaging
24 (EPI) was used to acquire a total of 170 scans per session, with a gradient EPI sequence.

1 The first three scans within each session were discarded to allow for T1 equilibration.
2 The scanning parameters were repetition time (TR), 2000 ms; echo time (TE), 30 ms;
3 flip angle (FA), 90°; field of view (FOV), 192 × 192 mm; matrix, 94 × 94; 35 axial
4 slices; and slice thickness, 3.0 mm with a 0.75 mm gap. T1-weighted anatomical
5 imaging with an MP-RAGE sequence was performed using the following parameters:
6 TR, 2300 ms; TE, 2.41 ms; FA, 8°; FOV; 256 × 256 mm; matrix, 256 × 256; 224 axial
7 slices; and slice thickness, 0.8 mm without a gap.

8

9 **Exclusion criteria for data**

10 For more accurate data analysis, we excluded some fMRI data based on the behavioral
11 criteria below.

12 a. The trial in which the participant moved the joystick before the execution phase in
13 execution sessions.

14 b. The trial in which the participant did not put the cursor in the target square at the end
15 of the execution phase in execution sessions.

16 c. The trial in which the participant moved the joystick to the wrong direction in
17 execution sessions, although the cursor was in the correct target square at the end of the
18 execution phase.

19 d. The trial in which participants chose “4 very poor” in the evaluation phase of imagery
20 sessions.

21

22 **Definition of regions of interest (ROIs)**

23 We defined motor-related regions as bilateral pre-SMA, SMA, and left M1, PMv using
24 Human Motor Area Template (Mayka et al., 2006), and left V1 was defined as

1 Brodmann Area 17. The activity of the left M1 reflected the movement of the right hand,
2 whereas the direction of movement of the right hand can also be classified in the left M1
3 (Ogawa & Inui, 2012). SMA and premotor cortex were associated with MI (Decety,
4 1996). Furthermore, PMv was related to hand actions (Rizzolatti et al., 2002). Pre-SMA
5 was also related to MI (Hanakawa et al., 2003), and pre-SMA was activated when the
6 cursor was unavailable during visual guided movement (Ogawa et al., 2006; Ogawa &
7 Inui, 2007).

8

9 **fMRI mass-univariate analysis**

10 Image preprocessing was performed using the SPM12 software (Wellcome Department
11 of Cognitive Neurology, <http://www.fil.ion.ucl.ac.uk/spm>). All functional images were
12 initially realigned to adjust for motion-related artifacts. Volume-based realignment was
13 performed by co-registering images using rigid body transformation to minimize the
14 squared differences between volumes. The realigned images were then spatially
15 normalized with the Montreal Neurological Institute template based on the affine and
16 nonlinear registration of coregistered T1-weighted anatomical images (normalization
17 procedure of SPM). They were resampled into 3-mm-cube voxels with the sinc
18 interpolation. Images were spatially smoothed using a Gaussian kernel of $6 \times 6 \times 6$ -mm
19 full width at half-maximum. However, images used for MVPA were not smoothed to
20 avoid blurring the fine-grained information contained in the multivoxel activity
21 (Kamitani & Sawahata, 2010; Mur et al., 2009; Ogawa et al., 2019). We analyzed
22 significantly activated areas during the ME or MI of right-hand movement compared
23 with activation during rest with univoxel analysis. Activation was the threshold at p
24 $< .05$, corrected for multiple comparisons for a family-wise error, with an extent

1 threshold of 10 voxels.

2

3 **Multivoxel pattern analysis**

4 In decoding analysis of MVPA, we classified the direction of hand movement in ME
5 and MI. The classification was performed based on a linear support vector machine run
6 by LIBSVM (<http://www.csie.ntu.edu.tw/~cjlin/libsvm>) with a fixed regularization
7 parameter $C = 1$. The beta value for each trial of voxels within ROIs (see Table 1) was
8 used as inputs to the classifier. ROI size did not affect the linear SVM's decoding
9 accuracy (Misaki et al., 2010). We attempted to interpret the direction of hand
10 movement in only ME (ME classification) or MI (MI classification) and between ME
11 and MI (cross-classification). Each participant attended three ME sessions and three MI
12 sessions. In ME classification and MI classification, we estimated the average
13 classification accuracy by a three-fold "leave-one-out" cross-validation, in which two
14 sessions were used as training and the remaining session was used as test data. In cross-
15 classification, the averaged classification accuracy was estimated via validation between
16 three ME sessions and three MI sessions (Table 2). Such cross-classification between
17 different task sets or stimuli has been used to investigate the activation pattern
18 similarities (Ogawa & Imai, 2016).

19 To compare spatial activation pattern similarities for different directions across
20 ME and MI, RSA (Kriegeskorte et al., 2008) was also conducted. Beta values of voxels
21 within ROIs were used as inputs to estimate the representational dissimilarity matrix
22 among the different directions of hand movement between ME and MI. There were a
23 total of 30 trials for each direction and modality (3 sessions \times 10 trials). Dissimilarity
24 was measured with cross-validated Mahalanobis distance (Ejaz et al., 2015), which

1 presents reliable dissimilarity metrics for RSA (Walther et al., 2016). To ensure
2 invertibility and stability, the voxel-by-voxel noise covariance matrix was separately
3 estimated within one dataset using an optimal shrinkage algorithm (Ledoit & Wolf,
4 2003). We then compared the off-diagonal elements of the representational dissimilarity
5 matrix, which represent the dissimilarity of activation patterns between different
6 modalities and directions.

7

8 **Results**

9 **Behavioral analysis**

10 According to the exclusion criteria, we excluded the error trials based on behavior data.
11 In a total of 60 trials of ME sessions and 60 trials of MI sessions, the percentage (SD) of
12 error trials per participant in ME and MI sessions was 2.78% (3.77%) and 2.12%
13 (3.18%), respectively.

14

15 **fMRI mass-univariate analysis**

16 We analyzed the activated regions of the brain using a univariate analysis of single
17 voxels and the regions that were significantly activated by comparing the modalities
18 (ME vs. MI) and the direction of movements (left vs. right). Activities between the left–
19 right directions in ME were compared. No areas significantly differed between the left
20 and right directions in ME at the corrected threshold of $p < .05$ and an extent threshold
21 of 10 voxels. Both left and right directions of the right hand moving revealed the
22 activations in the left M1 and left insula (Figure 3 and Table 3). Next, we compared the
23 activity during which the participants imagined the right hand moving between the left
24 and right directions. This comparison also revealed that no areas were significantly

1 differently activated between the left and right directions in MI. Both left and right
 2 directions of hand-moving imagery revealed the activations in the bilateral insula and
 3 SMA (Figure 3). Next, we compared the activated regions between the ME sessions and
 4 the MI sessions. Activations were found to be majorly in the left M1 and vermis during
 5 ME sessions and right M1 during MI sessions. There were no overlapped areas between
 6 “ME > rest” and “MI > rest” at the corrected threshold of $p < .05$ and an extent
 7 threshold of 10 voxels (Figure 4).

8

9 Next, ROI analysis was performed to compare the averaged parameter estimates
 10 (beta values) between the ME and MI sessions and the left and right directions.

11 Repeated measures analysis of variance was conducted with the modalities (ME and MI)
 12 and the hand movement directions (left and right) as within the subjects’ factors (Figure
 13 5). In both left M1 and bilateral SMA, a significant main effect was observed between
 14 the ME and MI (left M1, $F(1, 14) = 43.791, p < .001, \mu_p^2 = .758$; bilateral SMA, $F(1, 14)$
 15 $= 8.569, p = .011, \mu_p^2 = .380$) and also a significant interaction between the two factors
 16 (left M1, $F(1, 14) = 11.274, p = .005, \mu_p^2 = .446$; bilateral SMA, $F(1, 14) = 13.074, p$
 17 $= .003, \mu_p^2 = .483$). The beta value of the left M1 and bilateral SMA was significantly
 18 higher when the hand was moving to the left than the right in ME sessions (left M1, $F =$
 19 $8.132, p = .013$; bilateral SMA, $F = 12.149, p = .004$). In bilateral pre-SMA, there was
 20 no main effect but a significant interaction was observed ($F(1, 14) = 8.375, p = .012, \mu_p^2$
 21 $= .374$). In the right direction, the beta value of bilateral pre-SMA in the MI sessions
 22 was significantly higher than in the ME sessions ($F = 5.134, p = .040$). Also, in the ME
 23 sessions, the beta value of bilateral pre-SMA was significantly higher when the hand
 24 was moving to the left than the right ($F = 11.759, p = .004$).

1

2 **Multivoxel classification analysis**

3 We first conducted MVPA to classify the direction of ME by the subjects using the
4 activities of each ROI. In left M1, significantly higher-than-chance classification
5 accuracy was observed ($t(14) = 6.49, p < .001$, Cohen's $d = 1.68$). We also found
6 significantly higher-than-chance classification accuracies in bilateral pre-SMA ($t(14) =$
7 $3.38, p = .005$, Cohen's $d = .87$), SMA ($t(14) = 2.61, p = .021$, Cohen's $d = .67$), and left
8 PMv ($t(14) = 2.42, p = .030$, Cohen's $d = .62$), V1 ($t(14) = 11.89, p < .001$, Cohen's $d =$
9 3.07) (Figure 6A). Next, we conducted MVPA to classify the direction of MI. We found
10 significantly higher-than-chance classification accuracies in bilateral pre-SMA ($t(14) =$
11 $2.61, p = .010$, Cohen's $d = .77$) and left V1 ($t(14) = 3.29, p = .005$, Cohen's $d = .85$),
12 but no significant difference in bilateral SMA ($t(14) = -.87, p = .398$, Cohen's $d = -.23$)
13 and left M1 ($t(14) = 1.13, p = .277$, Cohen's $d = .29$), PMv ($t(14) = 1.07, p = .304$,
14 Cohen's $d = .28$) (Figure 6B).

15 We also conducted MVPA to classify the direction across ME and MI. We
16 found significantly higher-than-chance classification accuracies in left V1 ($t(14) = 5.87$,
17 $p < .001$, Cohen's $d = 1.52$). However, no significant difference in bilateral pre-SMA
18 ($t(14) = .44, p = .665$, Cohen's $d = .11$), SMA ($t(14) = -.15, p = .883$, Cohen's $d = -.04$)
19 and left M1 ($t(14) = .95, p = .358$, Cohen's $d = .25$), PMv ($t(14) = .31, p = .763$, Cohen's
20 $d = .08$) (Figure 6C). These results indicated distinct spatial activation patterns for the
21 movement directions between ME and MI in pre-SMA.

22

23 **Representational similarity analysis**

24 The RSA was used to investigate similarity in activation patterns of bilateral pre-SMA

1 and left V1 between different directions (left vs. right) across modalities (ME and MI,
2 Figure 7A). Because bilateral pre-SMA and left V1 were the only ROIs that were
3 significantly higher-than-chance in the ME classification and MI classification, a paired
4 sample t-test was conducted with the dissimilarity between the same direction but
5 different modalities (e.g., ME left and MI left) and different directions with different
6 modalities (e.g., ME left and MI right) across ME and MI for bilateral pre-SMA and left
7 V1 (Figure 7B). The result showed that different direction dissimilarities across ME and
8 MI was significantly higher than the dissimilarity of the same direction in left V1 with
9 null hypothesis significance testing, whereas there was no evidence for a difference
10 between the dissimilarities by Bayes factor ($t(29) = 2.06$, $p = .049$, Cohen's $d = .376$,
11 $BF_{10} = 1.221$). There was moderate evidence for no difference between the dissimilarity
12 of different directions across modalities and the dissimilarity of same direction across
13 modalities in bilateral pre-SMA ($t(29) = .33$, $p = .745$, Cohen's $d = .060$, $BF_{10} = .204$).

14

15 **Discussion**

16 This study investigated whether the different hand movement directions shared a similar
17 neural code in motor-related regions between ME and MI. We first analyzed activated
18 regions in the whole brain with conventional univoxel analysis within the ME and MI
19 sessions. During the execution phase of the ME session, significantly increased
20 activations were found in left M1 and left insula in both left and right directions. The
21 left M1 is well known for its role in right-hand movements (Sanes et al., 1995).
22 Contralateral insula activation has also been reported during voluntary limb movement
23 (Chollet et al., 1991) and finger movements (Fink et al., 1997). During the imagery
24 phase of the MI session, both left and right directions of hand moving imagery revealed

1 the activations in bilateral insula and SMA. A previous study indicated that SMA
2 activity was associated with MI (Decety, 1996). The comparison between left and right
3 direction hand movements in both ME and MI sessions showed no significant activated
4 areas. This result indicated that conventional univoxel analysis could not distinguish
5 differences in brain activity between the left and right directions of hand movements in
6 both ME and MI.

7 ROI analysis of the beta value revealed that left M1, SMA, and pre-SMA
8 activities were significantly higher during right hand moving to the left direction than
9 the right direction in ME sessions. The previous study showed that right hands that were
10 rotated in a clockwise direction were more difficult than when they were rotated in a
11 counterclockwise direction (de Lange et al., 2006). That might cause stronger activities
12 in left M1, SMA, and pre-SMA during the movement of the right hand to the left side.

13 Our multivoxel classification analysis in ME classification revealed that the
14 classification accuracies in bilateral SMA, pre-SMA, and left M1, PMv, and V1 were
15 significantly higher than the chance level. The left M1 and V1 result is consistent with
16 the previous study (Ogawa & Inui, 2012), which also classified the hand movement
17 directions while participants used a mouse. Bilateral SMA is associated with the
18 preparation and readiness for voluntary movements (Cunnington et al., 1996, 2003),
19 whereas PMv is related to hand actions (Rizzolatti et al., 2002). Pre-SMA is related to
20 visuomotor imagery (Deiber et al., 1998; Johnston et al., 2004; Leek & Johnston, 2009).
21 Previous studies showed that pre-SMA activates when visual feedback is unavailable
22 during visual guided movements (Ogawa et al., 2006; Ogawa & Inui, 2007). In the
23 present study, there was no visual feedback during ME sessions, the participants might
24 visually estimate cursor position during right-hand movement. Our multivoxel

1 classification analysis in MI classification revealed that significantly higher-than-chance
2 classification accuracy occurred only in bilateral pre-SMA and left V1, which showed
3 that V1 and pre-SMA were also related to hand movement direction in MI.

4 We conducted cross-classification to investigate whether the different hand
5 movement directions between ME and MI shared a similar neural code in bilateral pre-
6 SMA and left V1. We only found significantly higher-than-chance accuracy in left V1,
7 not in the bilateral pre-SMA. This result suggests that the activation of pre-SMA,
8 although related to both ME and MI, and the activity patterns in pre-SMA are separate
9 from each other. We conducted RSA to confirm this result further. The result of RSA
10 showed that the dissimilarity of different directions across ME and MI was significantly
11 higher than the dissimilarity of the same direction in left V1, and there was moderate
12 evidence for no difference between them in bilateral pre-SMA. Thus, the bilateral pre-
13 SMA did not share a similar neural code in hand movement direction across ME and MI.

14 MI is generally classified into two different types: kinesthetic type and visual
15 type (Jeannerod, 1995). Our participants might unconsciously imagine the trajectory of
16 the cursor movement while moving the joystick during the ME sessions. In the MI
17 sessions, the participants were instructed to imagine both the visual and kinesthetic
18 aspects of hand movement. Although visuomotor imagery was present in both ME and
19 MI sessions, the participants might have had difficulty visualizing the hand and cursor
20 movements simultaneously. This might be the reason why pre-SMA activation patterns
21 were different between ME sessions and MI sessions. Additionally, whereas pre-SMA
22 is related particularly to visuomotor imagery (Deiber et al., 1998), we cannot deny the
23 possibility that our participants primarily used the kinesthetic type of MI during MI
24 sessions, which might also allow pre-SMA to be decoded with significantly higher

1 accuracy than the chance level.

2

3 **Conclusion**

4 In summary, using multivariate analysis of fMRI activities, we found that pre-
5 SMA was the only motor-related region related to hand movement direction in both ME
6 and MI, but the activity patterns of ME and MI were distinct from each other.

7

8 **Glossary:**

9 motor execution, ME; motor imagery, MI; functional magnetic resonance imaging,
10 fMRI; presupplementary motor area, pre-SMA; multivoxel pattern analysis, MVPA;
11 representational similarity analysis, RSA; echo-planar imaging, EPI; repetition time, TR;
12 echo time, TE; flip angle, FA; field of view, FOV; regions of interest, ROIs.

13

14 **Funding:** This work was supported by JSPS KAKENHI Grant Numbers JP21H00958
15 & JP19H00634 to K.O and JST SPRING, Grant Number JPMJSP2119 to Y.Y. This
16 work was partially supported by Graduate Grant Program of Graduate School of
17 Humanities and Human Sciences, Hokkaido University.

18

19 **Acknowledgment:** The authors would like to thank Enago (www.enago.jp) for the
20 English language review.

21

22 **Declaration of Interest:** None.

23

24 **References:**

- 1 Brainard, D. H. (1997). The Psychophysics Toolbox. *Spatial Vision*, *10*(4), 433–436.
2 <https://doi.org/10.1163/156856897X00357>
- 3 Chollet, F., Dapierro, V., Wise, R. J. S., Brooks, D. J., Dolan, R. J., & Frackowiak, R. S.
4 J. (1991). The functional anatomy of motor recovery after stroke in humans: A
5 study with positron emission tomography. *Annals of Neurology*, *29*(1), 63–71.
6 <https://doi.org/10.1002/ana.410290112>
- 7 Cunnington, R., Iansek, R., Bradshaw, J. L., & Phillips, J. G. (1996). Movement-related
8 potentials associated with movement preparation and motor imagery. *Experimental*
9 *Brain Research*, *111*(3), 429–436. <https://doi.org/10.1007/BF00228732>
- 10 Cunnington, R., Windischberger, C., Deecke, L., & Moser, E. (2003). The preparation
11 and readiness for voluntary movement: A high-field event-related fMRI study of
12 the Bereitschafts-BOLD response. *NeuroImage*, *20*(1), 404–412.
13 [https://doi.org/10.1016/S1053-8119\(03\)00291-X](https://doi.org/10.1016/S1053-8119(03)00291-X)
- 14 de Lange, F. P., Helmich, R. C., & Toni, I. (2006). Posture influences motor imagery:
15 An fMRI study. *NeuroImage*, *33*(2), 609–617.
16 <https://doi.org/10.1016/j.neuroimage.2006.07.017>
- 17 Decety, J. (1996). The neurophysiological basis of motor imagery. *Behavioural Brain*
18 *Research*, *77*(1–2), 45–52. [https://doi.org/10.1016/0166-4328\(95\)00225-1](https://doi.org/10.1016/0166-4328(95)00225-1)
- 19 Deiber, M.-P., Ibañez, V., Honda, M., Sadato, N., Raman, R., & Hallett, M. (1998).
20 Cerebral Processes Related to Visuomotor Imagery and Generation of Simple
21 Finger Movements Studied with Positron Emission Tomography. *NeuroImage*,
22 *7*(2), 73–85. <https://doi.org/10.1006/nimg.1997.0314>
- 23 Ejaz, N., Hamada, M., & Diedrichsen, J. (2015). Hand use predicts the structure of
24 representations in sensorimotor cortex. *Nature Neuroscience*, *18*(7), 1034–1040.

- 1 <https://doi.org/10.1038/nm.4038>
- 2 Erdfelder, E., FAul, F., Buchner, A., & Lang, A. G. (2009). Statistical power analyses
3 using G*Power 3.1: Tests for correlation and regression analyses. *Behavior*
4 *Research Methods*, *41*(4), 1149–1160. <https://doi.org/10.3758/BRM.41.4.1149>
- 5 Faul, F., Erdfelder, E., Lang, A. G., & Buchner, A. (2007). G*Power 3: A flexible
6 statistical power analysis program for the social, behavioral, and biomedical
7 sciences. *Behavior Research Methods*, *39*(2), 175–191.
8 <https://doi.org/10.3758/BF03193146>
- 9 Fink, G. R., Frackowiak, R. S. J., Pietrzyk, U., & Passingham, R. E. (1997). Multiple
10 nonprimary motor areas in the human cortex. *Journal of Neurophysiology*, *77*(4),
11 2164–2174. <https://doi.org/10.1152/jn.1997.77.4.2164>
- 12 Grush, R. (2004). The emulation theory of representation: Motor control, imagery, and
13 perception. *Behavioral and Brain Sciences*, *27*(3), 377–396.
14 <https://doi.org/10.1017/S0140525X04000093>
- 15 Hanakawa, T. (2016). Organizing motor imageries. *Neuroscience Research*, *104*, 56–63.
16 <https://doi.org/10.1016/j.neures.2015.11.003>
- 17 Hanakawa, T., Dimyan, M. A., & Hallett, M. (2008). Motor Planning, Imagery, and
18 Execution in the Distributed Motor Network: A Time-Course Study with
19 Functional MRI. *Cerebral Cortex*, *18*(12), 2775–2788.
20 <https://doi.org/10.1093/cercor/bhn036>
- 21 Hanakawa, T., Immisch, I., Toma, K., Dimyan, M. A., van Gelderen, P., & Hallett, M.
22 (2003). Functional properties of brain areas associated with motor execution and
23 imagery. *Journal of Neurophysiology*, *89*(2), 989–1002.
24 <https://doi.org/10.1152/jn.00132.2002>

- 1 Hardwick, R. M., Caspers, S., Eickhoff, S. B., & Swinnen, S. P. (2018). Neural
2 correlates of action: Comparing meta-analyses of imagery, observation, and
3 execution. *Neuroscience and Biobehavioral Reviews*, *94*(December 2017), 31–44.
4 <https://doi.org/10.1016/j.neubiorev.2018.08.003>
- 5 Jeannerod, M. (1995). Mental imagery in the motor context. *Neuropsychologia*, *33*(11),
6 1419–1432. [https://doi.org/10.1016/0028-3932\(95\)00073-C](https://doi.org/10.1016/0028-3932(95)00073-C)
- 7 Jeannerod, M. (2001). Neural simulation of action: A unifying mechanism for motor
8 cognition. *NeuroImage*, *14*(1 II), 103–109. <https://doi.org/10.1006/nimg.2001.0832>
- 9 Johnston, S., Leek, E. C., Atherton, C., Thacker, N., & Jackson, A. (2004). Functional
10 contribution of medial premotor cortex to visuo-spatial transformation in humans.
11 *Neuroscience Letters*, *355*(3), 209–212.
12 <https://doi.org/10.1016/j.neulet.2003.11.011>
- 13 Kamitani, Y., & Sawahata, Y. (2010). Spatial smoothing hurts localization but not
14 information: Pitfalls for brain mappers. In *NeuroImage* (Vol. 49, Issue 3, pp. 1949–
15 1952). Academic Press Inc. <https://doi.org/10.1016/j.neuroimage.2009.06.040>
- 16 Kleiner, M., Brainard, D., & Pelli, D. (2007). What's new in Psychtoolbox-3?
17 *Perception* *36* *ECVP Abstract Supplement*, *36*(0), 14.
18 <https://doi.org/10.1068/v070821>
- 19 Kriegeskorte, N., Mur, M., & Bandettini, P. (2008). Representational similarity analysis
20 - connecting the branches of systems neuroscience. *Frontiers in Systems*
21 *Neuroscience*, *2*(NOV), 1–28. <https://doi.org/10.3389/neuro.06.004.2008>
- 22 Ledoit, O., & Wolf, M. (2003). Improved estimation of the covariance matrix of stock
23 returns with an application to portfolio selection. *Journal of Empirical Finance*,
24 *10*(5), 603–621. [https://doi.org/10.1016/S0927-5398\(03\)00007-0](https://doi.org/10.1016/S0927-5398(03)00007-0)

- 1 Leek, E. C., & Johnston, S. J. (2009). Functional specialization in the supplementary
2 motor complex. *Nature Reviews Neuroscience*, *10*(1), 78–78.
3 <https://doi.org/10.1038/nrn2478-c1>
- 4 Mayka, M. A., Corcos, D. M., Leurgans, S. E., & Vaillancourt, D. E. (2006). Three-
5 dimensional locations and boundaries of motor and premotor cortices as defined by
6 functional brain imaging: a meta-analysis. *NeuroImage*, *31*(4), 1453–1474.
7 <https://doi.org/10.1016/j.neuroimage.2006.02.004>
- 8 Misaki, M., Kim, Y., Bandettini, P. A., & Kriegeskorte, N. (2010). Comparison of
9 multivariate classifiers and response normalizations for pattern-information fMRI.
10 *NeuroImage*, *53*(1), 103–118. <https://doi.org/10.1016/j.neuroimage.2010.05.051>
- 11 Munzert, J., Lorey, B., & Zentgraf, K. (2009). Cognitive motor processes: The role of
12 motor imagery in the study of motor representations. *Brain Research Reviews*,
13 *60*(2), 306–326. <https://doi.org/10.1016/j.brainresrev.2008.12.024>
- 14 Mur, M., Bandettini, P. A., & Kriegeskorte, N. (2009). Revealing representational
15 content with pattern-information fMRI - An introductory guide. *Social Cognitive
16 and Affective Neuroscience*, *4*(1), 101–109. <https://doi.org/10.1093/scan/nsn044>
- 17 Ogawa, K., & Imai, F. (2016). Hand-independent representation of tool-use pantomimes
18 in the left anterior intraparietal cortex. *Experimental Brain Research*, *234*(12),
19 3677–3687. <https://doi.org/10.1007/s00221-016-4765-7>
- 20 Ogawa, K., & Inui, T. (2007). Lateralization of the Posterior Parietal Cortex for Internal
21 Monitoring of Self- versus Externally Generated Movements. *Journal of Cognitive
22 Neuroscience*, *19*(11), 1827–1835. <https://doi.org/10.1162/jocn.2007.19.11.1827>
- 23 Ogawa, K., & Inui, T. (2012). Reference frame of human medial intraparietal cortex in
24 visually guided movements. *Journal of Cognitive Neuroscience*, *24*(1), 171–182.

- 1 https://doi.org/10.1162/jocn_a_00132
- 2 Ogawa, K., Inui, T., & Sugio, T. (2006). Separating brain regions involved in internally
3 guided and visual feedback control of moving effectors: An event-related fMRI
4 study. *NeuroImage*, 32(4), 1760–1770.
5 <https://doi.org/10.1016/j.neuroimage.2006.05.012>
- 6 Ogawa, K., Mitsui, K., Imai, F., & Nishida, S. (2019). Long-term training-dependent
7 representation of individual finger movements in the primary motor cortex.
8 *NeuroImage*, 202(July 2018), 116051.
9 <https://doi.org/10.1016/j.neuroimage.2019.116051>
- 10 Pelli, D. G. (1997). The VideoToolbox software for visual psychophysics:
11 Transforming numbers into movies. In *Spatial Vision* (Vol. 10, Issue 4, pp. 437–
12 442). <https://doi.org/10.1163/156856897X00366>
- 13 Pilgramm, S., de Haas, B., Helm, F., Zentgraf, K., Stark, R., Munzert, J., & Krüger, B.
14 (2016). Motor imagery of hand actions: Decoding the content of motor imagery
15 from brain activity in frontal and parietal motor areas. *Human Brain Mapping*,
16 37(1), 81–93. <https://doi.org/10.1002/hbm.23015>
- 17 Rizzolatti, G., Fogassi, L., & Gallese, V. (2002). Motor and cognitive functions of the
18 ventral premotor cortex. *Current Opinion in Neurobiology*, 12(2), 149–154.
19 [https://doi.org/10.1016/S0959-4388\(02\)00308-2](https://doi.org/10.1016/S0959-4388(02)00308-2)
- 20 Sanes, J., Donoghue, J., Thangaraj, V., Edelman, R., & Warach, S. (1995). Shared
21 neural substrates controlling hand movements in human motor cortex. *Science*,
22 268(5218), 1775–1777. <https://doi.org/10.1126/science.7792606>
- 23 Walther, A., Nili, H., Ejaz, N., Alink, A., Kriegeskorte, N., & Diedrichsen, J. (2016).
24 Reliability of dissimilarity measures for multi-voxel pattern analysis. *NeuroImage*,

- 1 137, 188–200. <https://doi.org/10.1016/j.neuroimage.2015.12.012>
- 2 Weaverdyck, M. E., Lieberman, M. D., & Parkinson, C. (2020). Tools of the Trade
3 Multivoxel pattern analysis in fMRI: a practical introduction for social and
4 affective neuroscientists. *Social Cognitive and Affective Neuroscience*, 15(4), 487–
5 509. <https://doi.org/10.1093/scan/nsaa057>
- 6 Zabicki, A., de Haas, B., Zentgraf, K., Stark, R., Munzert, J., & Krüger, B. (2017).
7 Imagined and executed actions in the human motor system: Testing neural
8 similarity between execution and imagery of actions with a multivariate approach.
9 *Cerebral Cortex*, 27(9), 4523–4536. <https://doi.org/10.1093/cercor/bhw257>
- 10
- 11

1 **Tables**

2 Table 1: Number of ROIs' voxels in MVPA

| ROI | number of voxels (SD) |
|-------------------|-----------------------|
| left M1 | 925.73 (54.31) |
| bilateral pre-SMA | 598.80 (21.67) |
| bilateral SMA | 696.93 (10.82) |
| left PMv | 788.20 (30.23) |
| left V1 | 457.47 (14.63) |

3

4 Table 2: Training sets and test sets in multivoxel pattern classification

| Training sets | number of trials | Test sets | number of trials |
|-----------------------------|------------------|------------------|------------------|
| <i>ME classification</i> | | | |
| ME session 1&2 | 40 | ME session 3 | 20 |
| ME session 1&3 | 40 | ME session 2 | 20 |
| ME session 2&3 | 40 | ME session 1 | 20 |
| total | 120 | | 60 |
| <i>MI classification</i> | | | |
| MI session 1&2 | 40 | MI session 3 | 20 |
| MI session 1&3 | 40 | MI session 2 | 20 |
| MI session 2&3 | 40 | MI session 1 | 20 |
| total | 120 | | 60 |
| <i>Cross-classification</i> | | | |
| ME session 1,2&3 | 60 | MI session 1,2&3 | 60 |
| MI session 1,2&3 | 60 | ME session 1,2&3 | 60 |
| total | 120 | | 120 |

5

6 Table 3: Anatomical regions, peak voxel coordinates, and t-values of observed
7 activations.

| Anatomic region | voxels | MNI coordinates | t-value |
|-----------------|--------|-----------------|---------|
|-----------------|--------|-----------------|---------|

| | | x | y | z | |
|-------------------------------|-----|-----|-----|-----|-------|
| <i>Execution</i> | | | | | |
| L Precentral cortex | 153 | -33 | -28 | 62 | 12.67 |
| Postcentral cortex | | -33 | -22 | 50 | 12.37 |
| R Lingual gyrus | 37 | 21 | -79 | 2 | 12.58 |
| Calcarine sulcus | | 12 | -79 | 11 | 10.34 |
| Vermis | 107 | 3 | -61 | -13 | 11.63 |
| R Cerebellum | | 21 | -46 | -19 | 9.89 |
| L Insula | 35 | -39 | -4 | 11 | 11.35 |
| Rolandic operculum | | -48 | -1 | 5 | 9.32 |
| L Middle occipital gyrus | 13 | -15 | -95 | -1 | 10.19 |
| L Rolandic operculum | 13 | -45 | -28 | 17 | 9.27 |
| <i>Imagery</i> | | | | | |
| R SMA | 185 | 12 | 8 | 65 | 16.33 |
| L SMA | | 3 | 14 | 50 | 13.63 |
| L Superior parietal lobule | 44 | -21 | -67 | 53 | 15.04 |
| R Inferior frontal gyrus | 36 | 48 | 11 | 2 | 14.50 |
| Insula | | 42 | 5 | 2 | 11 |
| R Insula | 33 | 33 | 26 | -1 | 13.53 |
| R Fusiform | 79 | 33 | -61 | -10 | 13.05 |
| Lingual gyrus | | 18 | -76 | -7 | 12.02 |
| L Insula | 90 | -39 | 17 | 2 | 12.65 |
| L Precentral cortex | 14 | -54 | 8 | 23 | 11.4 |
| R Inferior frontal gyrus | 16 | 54 | 11 | 17 | 10.83 |
| L Supramarginal | 21 | -60 | -28 | 38 | 10.62 |
| R Precentral cortex | 71 | 39 | -13 | 56 | 10.61 |
| L Fusiform | 47 | -33 | -55 | -16 | 10.44 |
| Lingual gyrus | | -21 | -76 | -10 | 9.74 |
| L Middle frontal gyrus | 18 | -27 | -4 | 53 | 9.64 |
| <i>Execution > Imagery</i> | | | | | |
| L Postcentral cortex | 93 | -36 | -31 | 56 | 13.47 |
| Precentral cortex | | -39 | -19 | 59 | 8.81 |
| Vermis | 14 | 3 | -61 | -19 | 10.84 |
| <i>Imagery > Execution</i> | | | | | |
| R Precentral cortex | 41 | 36 | -19 | 53 | 13.27 |

Execution Left

| | | | | | |
|---------------------|-----|-----|-----|-----|-------|
| L Precentral cortex | 128 | -33 | -28 | 62 | 13.93 |
| Postcentral cortex | | -48 | -22 | 53 | 11.04 |
| R Lingual gyrus | 25 | 21 | -79 | 2 | 11.75 |
| Vermis | 95 | 3 | -61 | -16 | 10.72 |
| R Cerebellum | | 18 | -46 | -19 | 10.30 |
| L Insula | 15 | -42 | -4 | 8 | 9.65 |

Execution Right

| | | | | | |
|----------------------|-----|-----|-----|-----|-------|
| L Postcentral cortex | 144 | -33 | -22 | 50 | 13.00 |
| Precentral cortex | | -33 | -28 | 59 | 11.82 |
| L Insula | 36 | -39 | -4 | 11 | 12.61 |
| Rolandic operculum | | -48 | -1 | 5 | 10.35 |
| R Cerebellum | 38 | 33 | -52 | -22 | 10.62 |
| Vermis | 33 | 3 | -64 | -10 | 10.49 |
| L Lingual gyrus | 10 | -12 | -76 | -1 | 9.68 |

Imagery Left

| | | | | | |
|----------------------------|----|-----|-----|-----|-------|
| R Insula | 27 | 36 | 26 | -1 | 13.23 |
| R Inferior frontal gyrus | 25 | 48 | 11 | 2 | 11.71 |
| Insula | | 42 | 5 | -1 | 10.49 |
| L SMA | 49 | 3 | 14 | 50 | 11.37 |
| L Superior parietal lobule | 26 | -21 | -67 | 53 | 11.35 |
| L Insula | 50 | -36 | 17 | 2 | 10.52 |
| Inferior frontal gyrus | | -51 | 11 | 2 | 9.62 |
| R Lingual gyrus | 18 | 18 | -76 | -7 | 10.46 |
| R Precentral cortex | 10 | 36 | -7 | 50 | 10.28 |
| L Lingual gyrus | 30 | -21 | -76 | -7 | 10.10 |
| Fusiform | | -27 | -61 | -10 | 9.60 |
| R SMA | 10 | 12 | 8 | 65 | 10.01 |
| R Postcentral cortex | 11 | 48 | -19 | 44 | 9.67 |
| L Supramarginal | 10 | -60 | -31 | 41 | 9.66 |

Imagery Right

| | | | | | |
|----------------------------|-----|-----|-----|-----|-------|
| R Fusiform | 149 | 33 | -61 | -10 | 23.91 |
| Lingual gyrus | | 18 | -79 | -7 | 12.09 |
| L Superior parietal lobule | 80 | -27 | -61 | 44 | 15.66 |
| R SMA | 181 | 12 | 8 | 65 | 13.82 |
| L SMA | | 3 | 14 | 50 | 13.46 |
| L Insula | 76 | -33 | 23 | 8 | 13.59 |
| R Precentral cortex | 141 | 39 | -10 | 59 | 13.10 |

| | | | | | |
|--------------------------|----|-----|-----|-----|-------|
| Postcentral cortex | | 45 | -22 | 53 | 10.23 |
| L Fusiform | 72 | -33 | -58 | -16 | 11.87 |
| Lingual gyrus | | -18 | -79 | -10 | 10.21 |
| L Supramarginal | 24 | -60 | -31 | 38 | 11.77 |
| R Insula | 69 | 33 | 26 | 2 | 11.73 |
| Inferior frontal gyrus | | 48 | 11 | 2 | 11.51 |
| L Superior frontal gyrus | 19 | -21 | -1 | 68 | 10.32 |
| L Precentral cortex | 16 | -36 | -7 | 41 | 10.32 |
| L Inferior frontal gyrus | 15 | -51 | 11 | 20 | 9.58 |

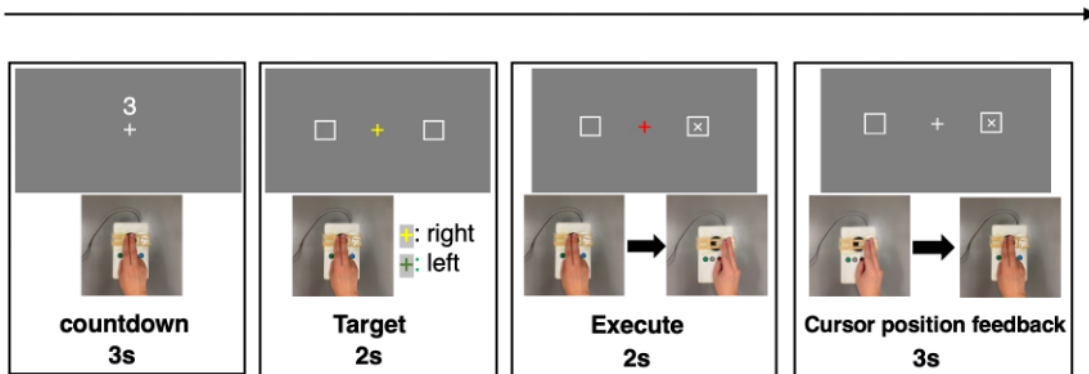
1

2 MNI, Montreal Neurological Institute; L, left hemisphere; R, right hemisphere.

3

4

5

1 **Figures**

2

3 **Figure 1:** Schematic depiction of the time course of a single trial in the practice session.

4 Each practice session included 10 trials. During the target phase, the order in which the

5 colors appear in the central fixation was random, and the same color would not appear

6 three consecutive times. The cursor is available to participants during the execution

7 phase only during the first practice session. The joystick can only be moved to the left

8 and right directions. Participants are instructed to move the joystick after the central

9 fixation turns red.

10

11



1

2 **Figure 2:** Schematic depiction of the time course of a single trial in ME session and MI

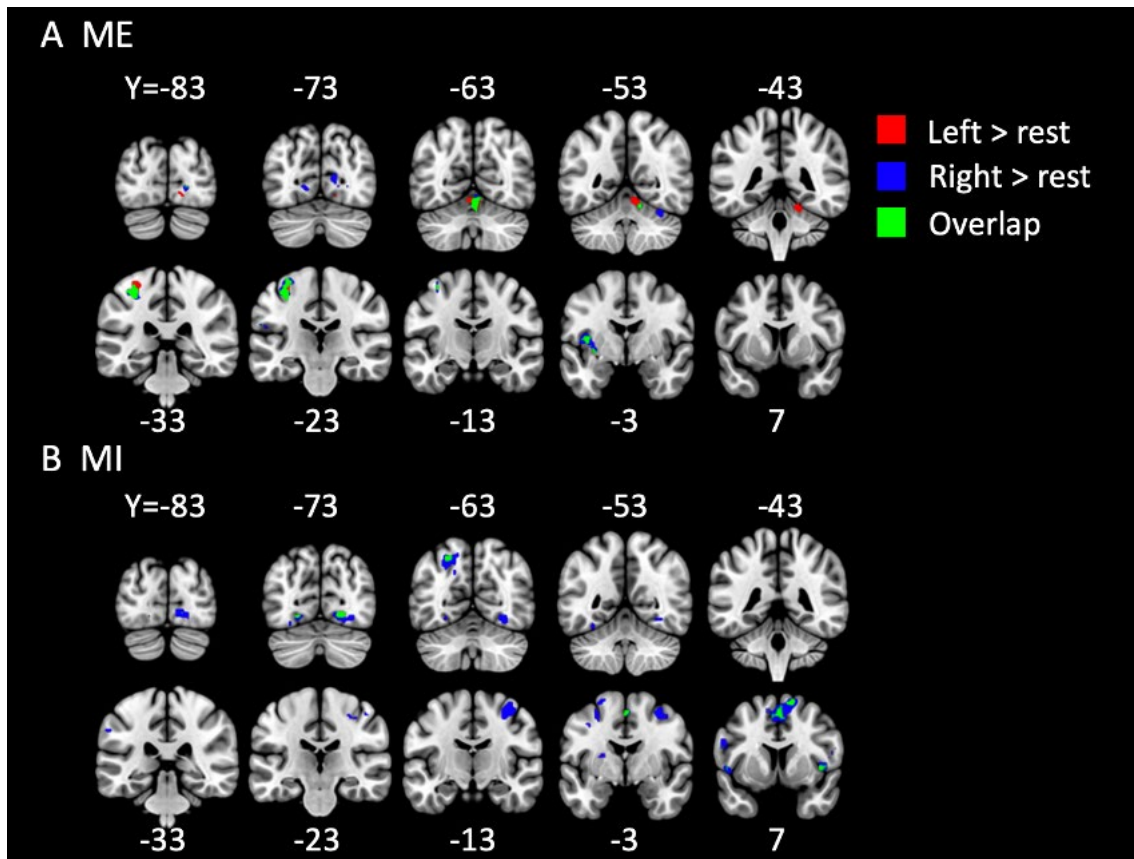
3 session. Each session included 20 trials. ME session was almost the same as practice

4 session 2, but the countdown phase changed to 9s. Participants were instructed to

5 evaluate the quality of the imagery after the picture of the hand appeared on the screen.

6

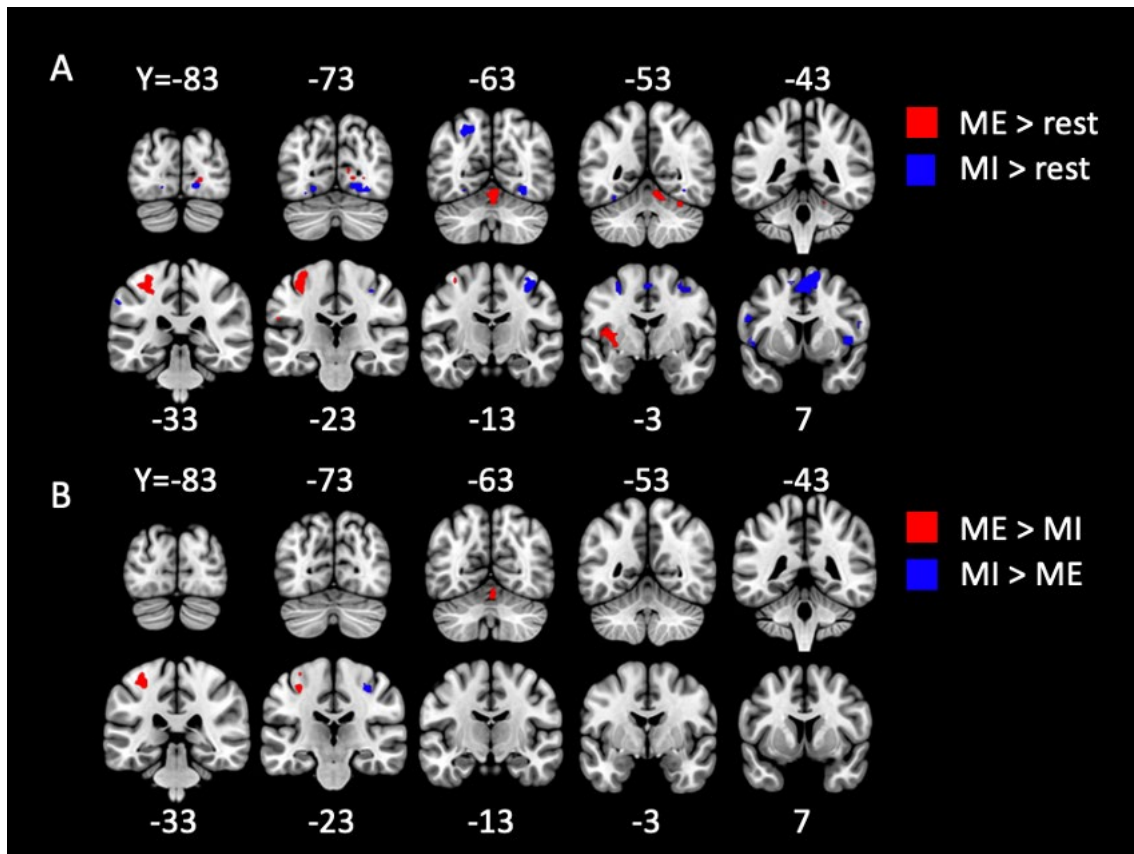
7



1

2 **Figure 3:** Activated regions in the fMRI univariate analysis of ME > rest (A) and MI >
 3 rest (B). Red showed only the left direction and blue showed only the left. Green
 4 regions were activated during both left and right directions.

5

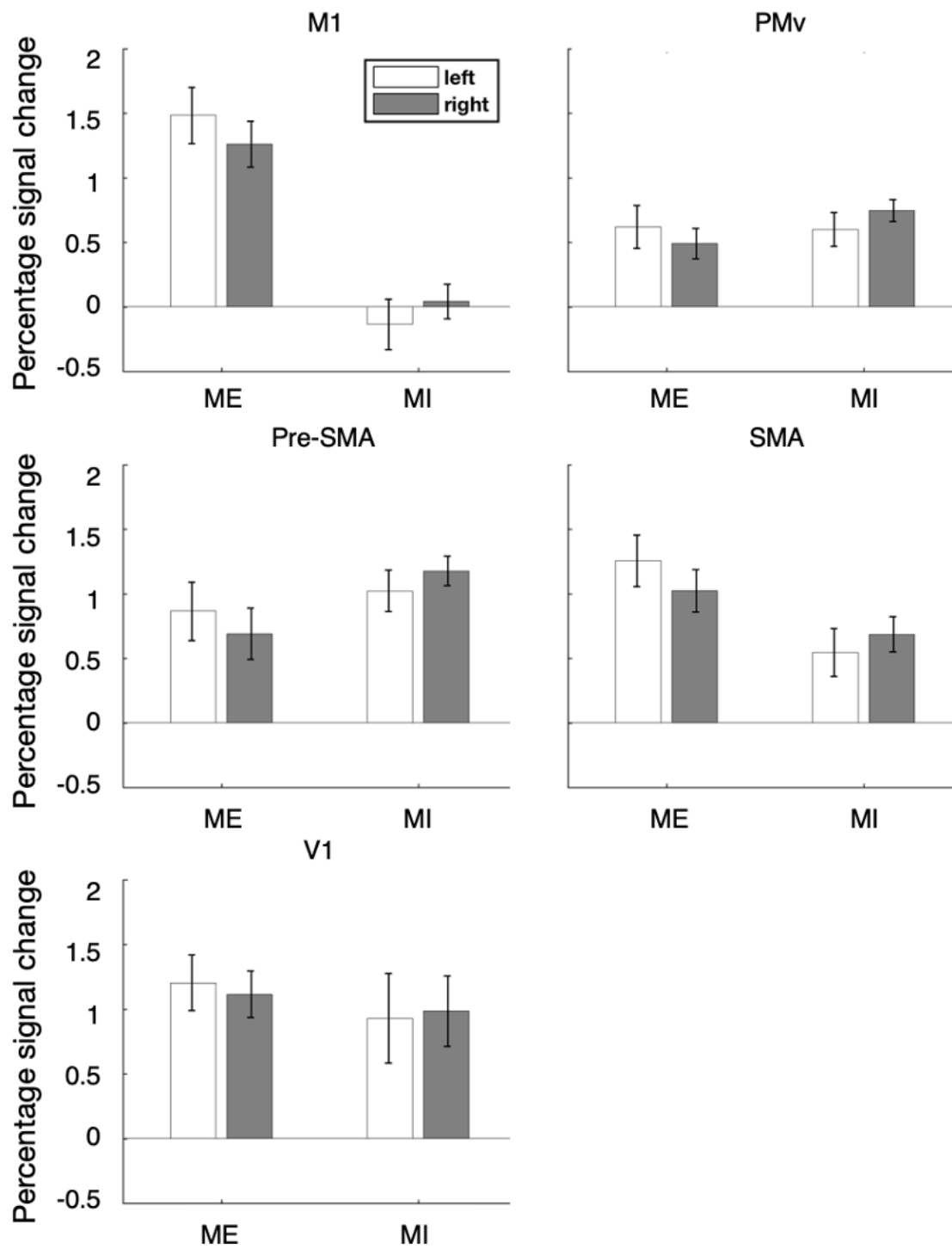


1

2 **Figure 4:** Activated regions in the fMRI univariate analysis of Task vs. Rest (A) and

3 ME sessions vs. MI sessions (B).

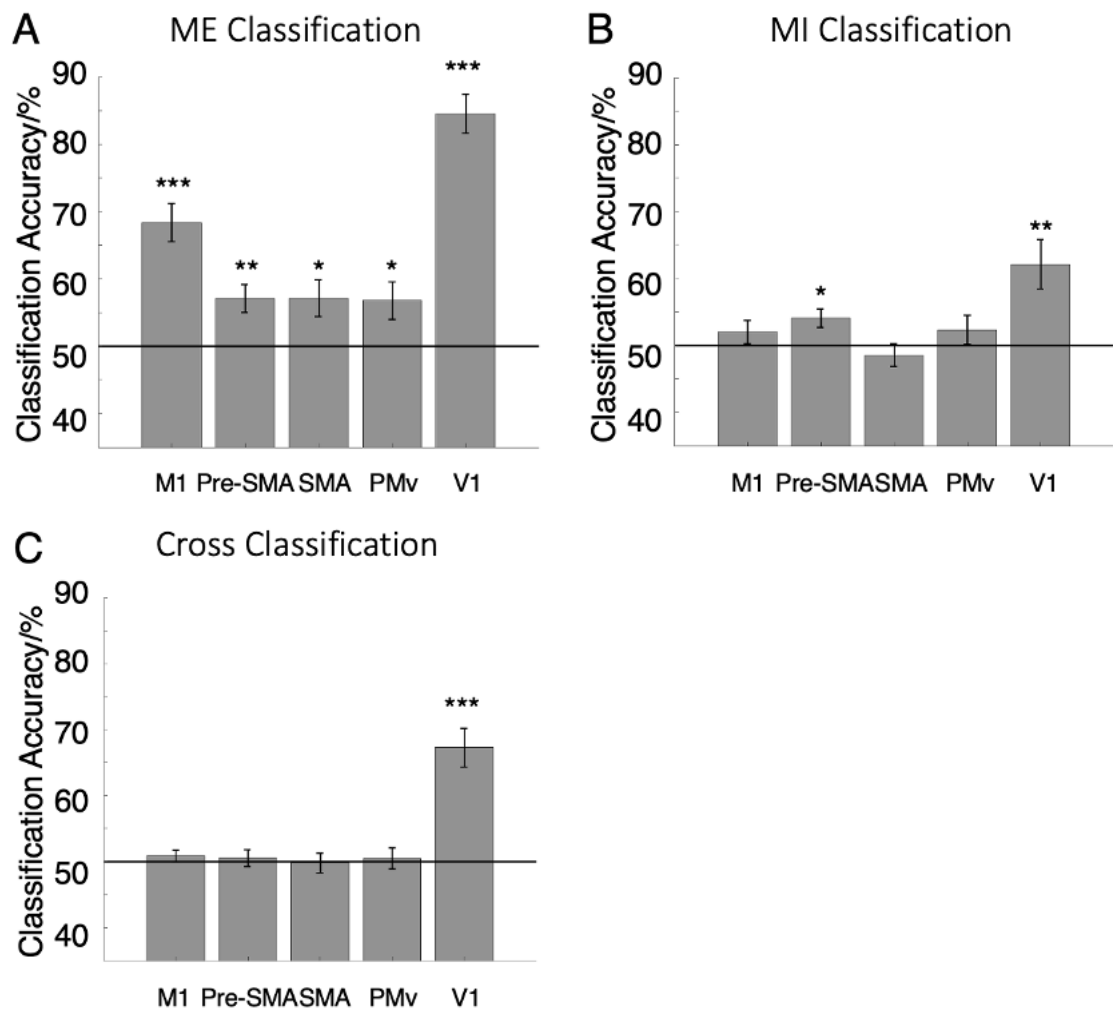
4



1

2 **Figure 5:** The averaged activation (beta value) within left M1, PMv, and bilateral pre-
 3 SMA, SMA, V1; error bars indicate SEMs.

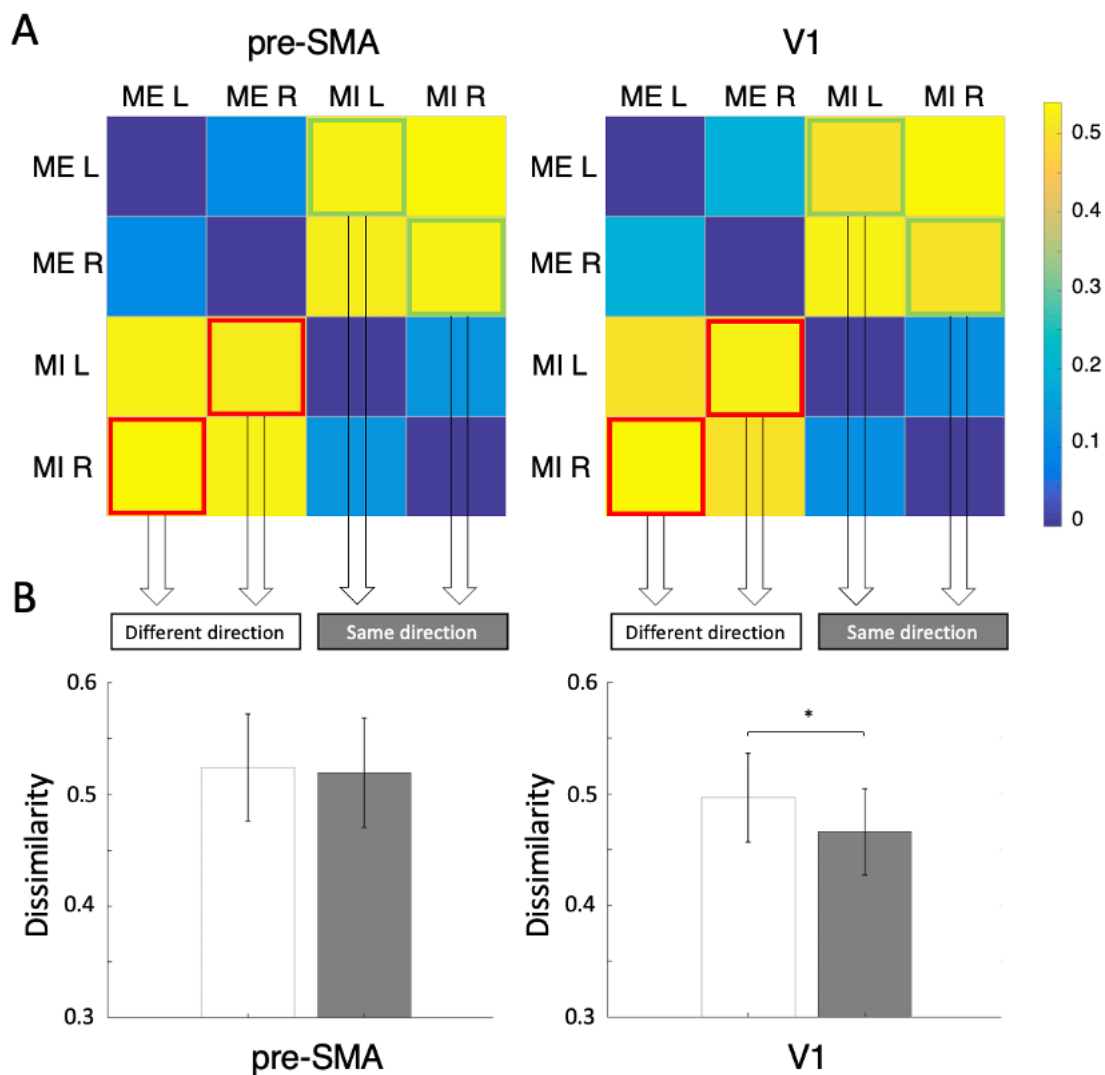
4



1

2 **Figure 6:** Classification accuracies with MVPA in ME classification (A), MI
 3 classification (B), and cross-classification (C) for movement directions in each ROI. (* p
 4 $< .05$, ** $p < .01$, and *** $p < .001$)

5



1

2 **Figure 7:** Representational similarity analysis (RSA) in bilateral pre-SMA and left V1.

3 Matrix squares show the representational dissimilarity matrix between different

4 directions and modalities, the blue rectangles show the dissimilarity between different

5 modalities but the same direction, and the red rectangles show the dissimilarity between

6 different modalities and different directions (A). The bar plots show the dissimilarities

7 of the same direction and different directions between different modalities; error bars

8 indicate SEMs (B). (* $p < .05$, ** $p < .01$, and *** $p < .001$).

9